Carbohydrate Polymers 196 (2018) 433–444

Contents lists available at ScienceDirect

Carbohydrate Polymers

journal homepage: www.elsevier.com/locate/carbpol

# Insights on the antifungal activity of amphiphilic derivatives of diethylaminoethyl chitosan against *Aspergillus flavus*

Amanda Manchini Dias[a], Marcia Perez dos Santos Cabrera[a,c], Aline Margarete Furuyama Lima[a], Sebastião Roberto Taboga[b], Patricia Simone Leite Vilamaior[b], Marcio José Tiera[a], Vera Aparecida de Oliveira Tiera[a,*]

[a] Departamento de Química e Ciências Ambientais, Universidade Estadual Paulista (Unesp), Instituto de Biociências Letras e Ciências Exatas (Ibilce), Câmpus São José do Rio Preto, R. Cristóvão Colombo, 2265, 15054-000, SP, Brazil

[b] Departamento de Biologia, Universidade Estadual Paulista (Unesp), Instituto de Biociências Letras e Ciências Exatas (Ibilce), Câmpus São José do Rio Preto, R. Cristóvão Colombo, 2265, 15054-000, SP, Brazil

[c] Departamento de Física, Universidade Estadual Paulista (Unesp), Instituto de Biociências Letras e Ciências Exatas (Ibilce), Câmpus São José do Rio Preto, R. Cristóvão Colombo, 2265, 15054-000, SP, Brazil

ARTICLE INFO

*Keywords:*
*Aspergillus flavus*
Amphiphilic chitosan derivatives
Antifungal
Inhibition
Cell wall impairment

ABSTRACT

In this study, the antifungal activity of chitosan derivatives against *A. flavus* was studied to understand the contribution of the molecular mass (Mw) and of the hydrophobic and electrostatic forces to the inhibition of fungal growth. The interaction of amphiphilics ranging from 8 to 130 kDa with model membranes of zwitterionic L-α-phosphatidylcholine (PC) and anionic L-α-phosphatidylcholine/L-α-phosphatidyl-DL-glycerol (PC:PG, 80:20 mol%) were exploited to obtain information on the inhibition mechanism. The results indicated that concurrent interactions control the antifungal activity. The decrease in the Mw weakens the self-association favoring the electrostatic and hydrophobic associations with the cell wall and anionic lipids of the lipid bilayer, indicating an increasing association of the amphiphilics with the fungal membrane. Laser confocal scanning microscopy of rhodamine labeled-derivatives and transmission electronic microscopy techniques showed that the amphiphilics affect the cell wall integrity by inducing the aggregation of hydrophobic constituents of the conidia.

## 1. Introduction

*Aspergillus flavus* has been considered a threat to human health due to its potential for causing invasive aspergillosis and infections, and due to its easy dispersion in the air leading to the contamination of agricultural crops, such as peanuts, maize and tree nuts, as well as oilseed crops (Hedayati, Pasqualotto, Warn, Bowyer, & Denning, 2007). The pathogenicity is mainly due to the production of carcinogenic aflatoxins, such as the aflatoxin B1, which is considered the most carcinogenic natural agent, capable of causing intoxication in bovine adults, domestic animals and implicated in hepatocellular carcinoma in humans (Chang & Ehrlich, 2010; Park & Troxell, 2002).

In the worldwide market of commercial pesticides the use of chemical fungicides corresponds to 17.5% (De, Borse, Kumar, & Mozundar, 2014). The mechanisms of action are varied, involving, for instance, the inhibition of proteins or the deregulation of ergosterol synthesis that consequently affects cell membranes. Moreover, to ensure greater efficacy, the use of a mix of active ingredients is common. The use of these chemical fungicides has caused great concern since they are classified as systemic and cumulative contaminants that are also potentially carcinogenic and teratogenic (Fakruddin, Chowdhury, Hossain, & Ahmed, 2015). Because of their indiscriminate use, increasingly resistant strains have been identified (Mortensen et al., 2010). Therefore, fungicides based on natural products (Bonilla & Sobral, 2016), essential oils (Nogueira et al., 2010) and plant defensins (Lacerda, Vasconcelos, Pelegrini, & de Sa, 2014) are very interesting options and the search for nontoxic compounds has recently driven the research in this field (Alkan & Yemenicioglu, 2016).

In this regard, chitosan has emerged as a promising antimicrobial agent, whose activity has been mainly attributed to the electrostatic interaction between its polycationic chains and the cell wall and cell membranes of the microorganisms (Kong, Chen, Xing, & Park, 2010; Sahariah & Másson, 2017). However, the efficiency of chitosan as an antimicrobial agent has been shown to depend not only on the target

* Corresponding author.
*E-mail addresses:* amanda_mdias@yahoo.com.br (A.M. Dias), cabrera.marcia@gmail.com (M.P. dos Santos Cabrera), amflima@gmail.com (A.M.F. Lima), taboga@ibilce.unesp.br (S.R. Taboga), patvila@ibilce.unesp.br (P.S.L. Vilamaior), mjt@ibilce.unesp.br (M.J. Tiera), verapoli@ibilce.unesp.br (V.A. de Oliveira Tiera).

https://doi.org/10.1016/j.carbpol.2018.05.032
Received 12 December 2017; Received in revised form 9 May 2018; Accepted 9 May 2018
Available online 20 May 2018
0144-8617/ 

microorganism but also on the intrinsic characteristics of the polysaccharide such as charge density, molecular weight (Mw), concentration, amphiphilicity and other physicochemical parameters like ionic strength, pH and temperature. Chitosan exhibits higher antimicrobial activity at low pH due to the protonation of its amino groups (Kong et al., 2010). The importance of positive charge density is supported by studies that used quaternized derivatives, which exhibited higher antimicrobial activity against bacteria (Ignatova, Starbova, Markova, Manolovaa, & Rashkov, 2006) and fungi (Pedro et al., 2013; Sajomsang, Gonil, Saesoo, & Ovatlarnporn, 2012; Souza et al., 2013) than plain chitosan. Besides the positive charge density, molecular weight and the hydrophilic/hydrophobic balance may also play an important role in the antimicrobial properties. The modification of the chitosan backbone through the grafting of alkyl chains (Rúnarsson et al., 2010) and aromatic groups (Tamera et al., 2017) has been shown to improve the antifungal and antibacterial activities of chitosan. It suggests that this improvement may result from the interaction of the amphiphilic chain with cell membrane phospholipids (Huang, Du, Zheng, Liu, & Fan, 2004; Rúnarsson et al., 2010). The antimicrobial activity of chitosan depends either on the type of microorganism or on molecular weight (Li, Chen, Liu, Zhang, & Tang, 2011). For instance, chitosans of low Mw showed higher antimicrobial activity against *Candida species* (Kulikov et al., 2014; Seyfarth et al., 2008) than those of high Mw (Tayel et al., 2010). Nevertheless, a fine-tuning on Mw is needed to achieve more effective molecules (Kulikov et al., 2014).

The Mw effect and the insertion of hydrophobic groups in the chitosan backbone are currently under investigation. However, further efforts in the investigation of the characteristics of the mechanism of action against fungi are required. Among them, the interactions with the cell wall components, the permeabilization of the fungal plasma membrane (Palma-Guerrero et al., 2010) and also the results of interactions of chitosan with cytoplasmic constituents (Goy & Assis, 2009). In particular, the mechanism by which amphiphilic chitosans exert their activity is not completely understood and investigations in this regard are pivotal for the preparation of effective antifungal agents.

Recently it has been demonstrated that amphiphilic derivatives of diethylaminoethyl chitosans have a significant antifungal activity against *A. flavus* and *A. parasiticus*. In general, the results showed that the antifungal activity was strongly dependent on Mw, hydrophobic groups content and polymer concentration (Gabriel, Tiera, & Tiera, 2015; Souza et al., 2013). The findings indicated that amphiphilic chitosans are more effective if they have either high Mw and lower hydrophobicity or low Mw and higher hydrophobicity.

In this current work, the main purpose was to gain insights into the mechanism of the antifungal activity of amphiphilic derivatives of chitosan against *A. flavus*, which could be related to the cell wall and cell membrane impairment. By varying the Mw, the role of hydrophobic interactions on the antifungal activity could be better clarified. A series of derivatives of varied Mw having fixed contents of diethylaminoethyl (DEAE) and hydrophobic groups were synthesized and characterized. The antifungal activities of these derivatives were tested against *A. flavus* and their interaction with model membranes made of phosphatidylcholine (PC) and phosphatidylcholine-phosphatidylglycerol (PC:PG) was studied (Lohner & Prenner, 1999; Palma-Guerrero et al., 2010). Additionally, laser scanning confocal microscopy and transmission electron microscopy were employed to evaluate structural modifications in the cell wall.

## 2. Experimental part

### 2.1. Materials

Commercial chitosan (CHC) with a degree of deacetylation (DD) of 85% (Polymar, Fortaleza, Brazil) was deacetylated to generate a highly deacetylated sample with DD of 97%. Sodium acetate, acetic acid, and sodium hydroxide were purchased from Synth (Diadema, Brazil). 2-Chloro-*N*,*N*-diethylethylamine hydrochloride (DEAE), deuterium chloride (35%) in deuterium oxide, deuterium oxide, 5,6-carboxyfluorescein (CF), egg L-α-phosphatidylcholine (PC) and egg L-α-phosphatidylglycerol sodium salt (PG) were purchased from Sigma-Aldrich Chemical Co. (São Paulo, Brazil). Potato dextrose agar (PDA) was purchased from Acumedia Manufacturers, Inc. (Lansing, USA). Water was deionized using a Gehaka water purification system. Spectra/Pore membranes (Spectrum) were employed for dialysis. All solvents were of reagent grade and used as received.

### 2.2. Synthesis of the amphiphilic derivatives of diethylaminoethyl chitosan of varied molecular weight (DEAE-$CH_{Dod}$)

The amphiphilic derivatives were synthesized in a two-step process using the highly deacetylated chitosan (CH, DD 97%) as starting material. First, CH was modified with 2-Chloro-*N*,*N*-diethylethylamine hydrochloride (DEAE) at pH 8.0, as previously described (Gabriel et al., 2015), to generate a derivative with a degree of substitution of about 40%. This first derivative was subsequently degraded by sodium nitrite in acetic acid solution (Huang, Khor, & Lim, 2004; Tømmeraas, Vårum, Christensen, & Smidsrød, 2001). To obtain DEAE-CH derivatives with varied molecular weights (Mw), the molar ratio of $NaNO_2$/glucosamine was varied from 0.02 to 0.38 (Table 1). Next, the samples of varied Mw were recovered by lyophilization and subjected to alkylation with dodecyl aldehyde followed by reduction with sodium borohydride (Desbrieres, Martinez, & Rinaudo, 1996; Souza et al., 2013) to reach a degree of substitution of 0.2 (Fig. 1a).

### 2.3. Characterization of the amphiphilic derivatives

The DEAE-CH derivatives were characterized by proton nuclear magnetic resonance ($^1$H NMR) and gel permeation chromatography

**Table 1**
Reaction conditions and physico-chemical properties of chitosan and its amphiphilic derivatives.

| Polymer | [a]MR Dodecyl/$NH_2$ | [b]MR DEAE/$NH_2$ | $^+DS_{DEAE}$ (%) | $^{++}DS_{Dod}$ (%) | [c]$MR_D$ $NaNO_2$/CH | Mw | Mw/Mn | CAC (g $L^{-1}$) | $DS_{RHODAMINE}$ (%) |
|---|---|---|---|---|---|---|---|---|---|
| $CH_{130(DD^a = 97\%)}$ | – | – | – | – | – | 122.4 | 2.93 | – | – |
| DEAE-CH | – | 0.5 | 40 | – | – | 136.5 | 2.97 | 0.069 | 0.85 |
| DEAE-$CH_{136}$-Dod | 0.22 | 0.5 | 40 | 19.3 | – | 136.5 | 2.97 | 0.004 | 0.52 |
| DEAE-$CH_{116}$-Dod | 0.22 | 0.5 | 40 | 19.3 | 0.02 | 116.1 | 2.81 | 0.006 | 0.82 |
| DEAE-$CH_{70}$-Dod | 0.22 | 0.5 | 40 | 18.7 | 0.09 | 69.0 | 2.54 | 0.009 | 0.78 |
| DEAE-$CH_{25}$-Dod | 0.22 | 0.5 | 40 | 18.3 | 0.21 | 25.3 | 2.92 | 0.013 | 0.79 |
| DEAE-$CH_8$-Dod | 0.22 | 0.5 | 40 | 20.3 | 0.38 | 8.7 | 3.08 | 0.021 | 2.67 |

$DS_{DEAE}$ = Degree of substitution by DEAE groups; $++DS_{Dod}$ = Degree of substitution by dodecyl groups; Mw = Molecular weight (kDa); Mw/Mn = Polydispersity; CAC = Critical Aggregation Concentrations (g $L^{-1}$).

[a] DD = Degree of deacetylation.

[b] MR = Molar ratios of DEAE and dodecyl aldehydes employed for the synthesis.

[c] $MR_D$ = molar ratios of sodium nitrite employed for degradation.

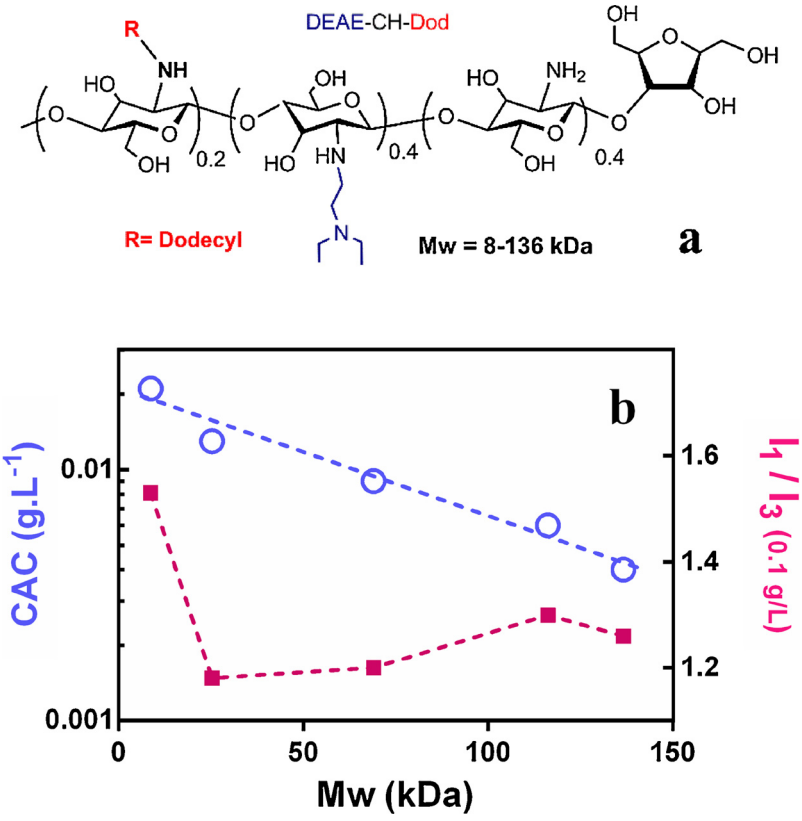


**Fig. 1.** a) Structure of the amphiphilic derivatives of varied molecular weights b) Critical aggregation concentrations (CAC, blue line) and $I_1/I_3$ ratio of pyrene (pink line, at 0.1 g $L^{-1}$ of polymer) as a function of amphiphilic Mw. Data represent the average of two independent experiments. (For interpretation of the references to colour in this figure legend, the reader is referred to the web version of this article.)

(GPC) techniques. Samples for $^1$H NMR analysis were prepared as previously described (Tiera et al., 2006) and the spectra were recorded using an Avance III HD 400 MHz spectrometer (Bruker, Billerica, USA).

GPC measurements were performed using an LC20 liquid chromatograph (Shimadzu, Kyoto, Japan) equipped with a RID-10A refractive index detector (Shimadzu, Kyoto, Japan) using Shodex OHpak SB-803 HQ and OHpak SB-805 HQ columns (Showa Denko K.K., Tokyo, Japan) and pullulan standards from 805 to 6.2 kDa. GPC analysis was carried out with the mobile phase of acetic acid 0.3 mol $L^{-1}$/sodium acetate 0.2 mol $L^{-1}$ and a flow rate of 0.8 mL/min at 35 °C (Gabriel et al., 2015).

### 2.4. Rhodamine-labelled chitosans

To observe the interaction of chitosan and its amphiphilic derivatives with *A. flavus* by confocal microscopy, compounds were labeled with a rhodamine isothiocyanate derivative using a previously reported procedure (Casé et al., 2009). To determine the labeling efficiency, solutions of the rhodamine-labeled compounds were prepared in an acetic acid buffer/methanol mixture (v/v) at pH 4.5 and the absorbance measured at 554 nm. A calibration curve was prepared with solutions ranging from $3.5 \times 10^{-6}$ to $2 \times 10^{-5}$ mol.$L^{-1}$ using a stock solution of rhodamine derivative (0.93 mg/10 mL). The degrees of labeling varied from 0.85% to 2.67% of substituted amino groups (Table 1).

### 2.5. Self-association: determination of the critical aggregation concentrations (CAC)

The self-association study of the chitosan amphiphilics was performed according to De Oliveira, Tiera, and Neumann (1996). Stock solutions of the polymers were injected into a buffer solution of $20 \times 10^{-3}$ mol $L^{-1}$ acetic acid/acetate, pH 5.5 and ionic strength of $150 \times 10^{-3}$ mol $L^{-1}$, containing pyrene at a concentration of $5 \times 10^{-7}$ mol $L^{-1}$, under magnetic stirring. The final concentration of amphiphilics ranged from $1 \times 10^{-4}$ to 0.8 gl $L^{-1}$. The ratio between the fluorescence intensities of peaks I (372.4 nm) and III (384 nm) of the emission spectrum of pyrene ($I_1/I_3$ ratio) was used to evaluate the polarity of the local environment and to determine the CAC. The measurements were made on an F-4500 spectrofluorometer (Hitachi, Tokyo, Japan) at 25 °C. Pyrene was excited at 310 nm and the spectra registered from 350 to 500 nm. The $I_1/I_3$ ratios of the spectra were used to graphically determine the critical aggregation concentrations (CAC)

### 2.6. Preparation of large unilamellar vesicles (LUVs)

LUVs made of PC and PC:PG 80:20 mol% were prepared from respective stock solutions as previously described (Cabrera et al., 2008). Briefly, aliquots of the phospholipid solutions were evaporated to render thin films free from solvent. These lipid films were hydrated with appropriate buffers (either $20 \times 10^{-3}$ mol $L^{-1}$ acetic acid/acetate buffer, pH 5.5, ionic strength $150 \times 10^{-3}$ mol.$L^{-1}$, for zeta potential and DLS experiments or Tris/HCl buffer containing $1 \times 10^{-3}$ mol $L^{-1}$ $Na_2EDTA$ and $25 \times 10^{-3}$ mol $L^{-1}$ CF, pH 7.4, for the CF-release experiments), vortexed and extruded rendering LUV dispersion of the desired concentration and of 100–120 nm diameter, as determined by DLS. LUVs containing entrapped carboxyfluorescein (CF) were obtained using the same procedure and the free CF was separated using a Sephadex G25 gel (GE Healthcare, Pittsburgh, USA) in a PD-10 column, eluted with the Tris-HCl buffer, pH 7.4. Lipid concentration was confirmed by phosphorus analysis (Rouser, Fleischer, & Yamamoto, 1970). LUV dispersions were kept under refrigeration (8 °C) and used within 24 h.

### 2.7. Interaction of CH and its derivatives with PC and PC:PG LUVs monitored by DLS

PC and PC:PG model membranes were used to mimic the fungal membrane of *A. flavus*, whose lipid composition is formed mainly by the zwitterionic lipid PC and the anionic lipid phosphatidylinositol (Dennison, Morton, Harris, & Phoenix, 2014). Stock solutions of

chitosan and derivatives were prepared in the same buffer as for LUVs ($20 \times 10^{-3}$ mol $L^{-1}$ acetic acid/acetate buffer, pH 5.5, ionic strength $150 \times 10^{-3}$ mol $L^{-1}$) and injected under gentle magnetic stirring into $1 \times 10^{-3}$ L ($1 \times 10^{-3}$ mol $L^{-1}$) of PC or PC:PG (80:20) LUVs. The final concentration of the polymers ranged from 0.005 to 1.0 g $L^{-1}$ and the measurements were taken after 30 min of gentle magnetic stirring. Size and zeta potential measurements were taken in a Zetasizer Nano ZS (Malvern Instruments, Malvern, U.K.), performed in duplicate with 3 accumulations for each measurement and the average values were used.

### 2.8. Carboxyfluorescein release study

The release of carboxyfluorescein (CF) was taken as a qualitative evaluation of the membrane permeability after incubation with chitosan and its amphiphilic derivatives. A suspension of CF-entrapped PC:PG LUVs at a concentration of $1 \times 10^{-3}$ mol $L^{-1}$ was obtained by dilution with $10 \times 10^{-3}$ mol $L^{-1}$ TRIS-HCl buffer, pH 7.4. An aliquot of CH or its amphiphilic derivatives was added into PC:PG dispersion to obtain mixtures with increasing polymer concentrations. The fluorescence intensity of CF was monitored at 15 min intervals at 520 nm and compared to dispersions lysed by the addition of 20 μL of 10% Triton X-100 solution (w/w). Experiments were conducted in a PC1 spectrofluorometer (ISS, Urbana Champaign, USA), at 25 °C, using a 1 cm quartz cell with excitation wavelength set at 490 nm.

### 2.9. Fungal strains and culture conditions

The antifungal activities of deacetylated chitosan (CH), DEAE40-CH and its amphiphilic derivatives were tested against *A. flavus*. The strains used were kindly provided by the Brazilian Collection of Microorganisms from the Environment and Industry (CBMAI; Campinas, Brazil) and were maintained on PDA (200 g/L potato infusion, 20 g/L dextrose, and 15 g/L agar) in the dark at 25 ± 2 °C.

### 2.10. Antifungal assays

Solutions of chitosan and derivatives were prepared by dissolving appropriate amounts of polymers in 50 mL acetic acid aqueous solution (1.0% w/w). The pH was adjusted to 5.0 and added to sterilized melted culture medium of PDA in deionized water (10% w/w) to obtain final concentrations of 0.1, 0.25, 0.50, 0.75 and 1.0 g $L^{-1}$. The culture media containing increased polymer concentrations were transferred to Petri dishes. After solidification, the Petri dishes were inoculated with $2 \times 10^{-6}$ L of spores previously counted in a Neubauer chamber. The inhibition indices of all polymers on the mycelial growth of *A. flavus* were determined as described by Souza et al. (2013) on the third day of cultivation as follows:

$$\text{Antifungal Index (\%)} = 1 - (Da/Db) \times 100$$

where Da is the diameter of the growth zone in the test plates and Db is the growth zone in the control plate. All data were expressed as mean ± S.E.M. Significant differences between groups were determined using Two-way ANOVA with Tukeý́s multiple comparison test. All statistical comparisons were made using GraphPad Prism 6.01 (GraphPad Software Inc., San Diego, CA, USA) and values of $P < 0.05$ were considered to be statistically significant.

### 2.11. Laser scanning confocal microscopy

To evaluate the interaction of the amphiphilics with *A. flavus,* the fungus was grown in the presence of the rhodamine-labeled derivatives. The slides used in the microscopy were prepared according to the adaptation of the Agar Block method described by Saggiorato et al. (2012), where culture medium cubes (PDA) solidified in the presence and absence of rhodamine-labeled chitosan derivatives (0.5 g $L^{-1}$) were inoculated with $1 \times 10^6$ spores of the fungus. Subsequently, they were deposited on a sterile microscopy plate, covered by a sterile cover slip and then incubated for 3 days at 25 °C. The slide and the coverslip with the adhered hyphae were then fixed using methanol and labeled using DAPI for the control hyphae (grown in the absence of any polymer) according to the DAPI Protocol for Fluorescence Imaging (DAPI Protocol, 2018). Images were taken using an LSM 710 Confocal Scanning Microscope (Zeiss, Oberkochen, Germany).

### 2.12. Transmission electron microscopy: ultrastructural analysis

The hyphae of the fungus grown in the absence and presence (0.5 g $L^{-1}$) of the chitosan derivatives for 3 days were fixed by immersion in 3% glutaraldehyde plus 0.25% tannic acid solution in Millonig's buffer, pH 7.3, containing 0.54% glucose (w/w) for 24 h. After washing with the same buffer, samples were post-fixed with 1% (w/w) osmium tetroxide for 1 h, washed in buffer, dehydrated in a graded acetone series and embedded in Araldite resin. Copper grids with ultrathin sections (50–75 nm) were prepared using a diamond knife and stained with 2% alcoholic uranyl acetate (w/w) for 30 min (Cotta-Pereira, Guerra, & Bittencourt-Sampaio, 1976), followed by 2% lead citrate in a 1 mol $L^{-1}$ sodium hydroxide solution for 10 min. Samples were evaluated by transmission electron microscopy using a LEO 906 TEM (Zeiss, Oberkochen, Germany) at 80 Kv.

## 3. Results and discussion

### 3.1. Synthesis and characterization of amphiphilic derivatives with varied Mw

The synthesis was planned to obtain amphiphilic derivatives with a fixed content of hydrophobic groups and varied molecular weights. The first step was carried out using CH, DD 97%, which was further modified to obtain a first derivative containing only diethylaminoethyl groups with a DS of about 40% (Fig. S1, Supplementary Materials). DEAE-CH derivatives ($DEAE_{40}$-CH) in the range of 8–130 kDa were obtained by degradation with sodium nitrite. GPC traces showed sigmoidal distributions (Fig. S2, Supplementary Materials) with similar polydispersities (Table 1). These derivatives were subsequently modified with dodecyl groups to achieve a fixed hydrophobic group content for all derivatives. Table 1 shows that the insertion of dodecyl chains was well controlled and degrees of substitution remained around 20%. Owing to their amphiphilic nature, intramolecular and intermolecular interactions dominate their aqueous solution behavior. Hence, as determined by pyrene fluorescence, the critical aggregation concentration (CAC) increased by about 5 times as Mw was decreased from 130 to 8 kDa (Fig. 1c and Fig. S3, Supplementary Materials). As the degree of substitution was kept constant, the decreasing CAC values indicate that longer polymer chains are more prone to form intra- and intermolecular aggregates. Moreover, above the CAC (0.1 g $L^{-1}$), the $I_1/I_3$ ratio, which reports the polarity in the core of aggregates, showed that only the lower Mw amphiphilic (8 kDa) exhibited more polar aggregates, confirming the weaker hydrophobic interactions. However, at higher concentrations, the aggregate becomes more hydrophobic and similar $I_1/I_3$ ratios in the range from 1.2 to 1.3 were obtained (Fig. 1c). Interestingly, even the derivative exclusively substituted with DEAE groups exhibited a tendency to self-assemble above 0.1 g/L, as denoted by the break in the curve of $I_1/I_3$. This indicates that ethyl groups of tertiary amines confer a certain amphiphilicity to the polycation chain (Fig. S3, Supplementary material).

### 3.2. Effect of the amphiphilic structure on mycelial growth of Aspergillus flavus

To investigate the effects of hydrophobic interactions and molecular weight on the inhibition of growth of *A. flavus*, the fungus was

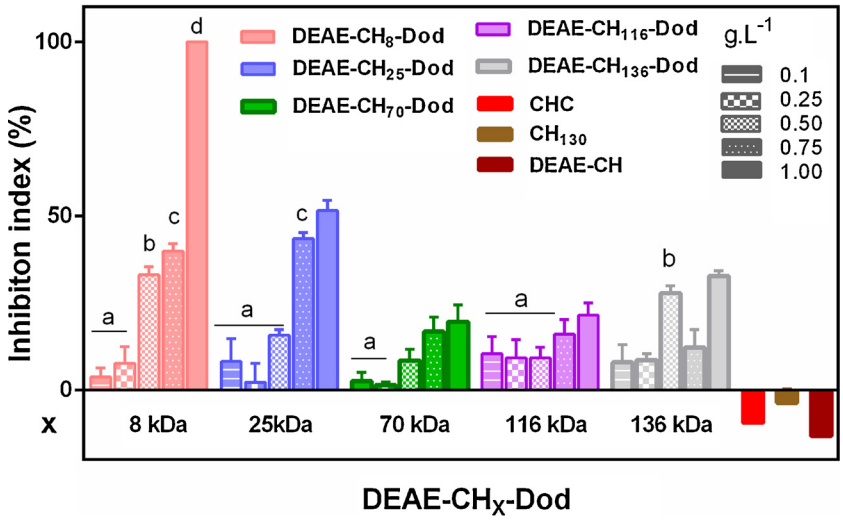


**Fig. 2.** Effect of amphiphilics molecular weight on the inhibition index of *A. flavus* at increasing concentrations. Vertical bars with different letters indicate significant differences according to the two-way ANOVA with Tukeýs multiple comparison test ($P < 0.05$).

inoculated in a culture medium containing increasing concentrations of the amphiphilics. At the lower polymer concentrations tested (0.1 and 0.25 g $L^{-1}$), the inhibition indexes, as measured by the radial growth of the colony, remained around 10% and increased in a concentration-dependent manner (Fig. 2 and Fig. S4). Moreover, the inhibition showed a clear dependence on Mw, and the lower Mw derivative (DEAE-$CH_8$-Dod) was more effective, completely inhibiting the growth of *A. flavus* at 1.0 g $L^{-1}$. However, for CHC, CH, and its hydrophilic derivative DEAE-CH, at the same concentration of 1.0 g $L^{-1}$, no inhibition was observed. Chitosan has been reported to exhibit antifungal activity against some fungi of the genus *Aspergillus*, such as *A. niger* (Plascencia-Jatomea, Viniegra, Olayo, Castillo-Ortega, & Shirai, 2003) and *A. parasiticus* (Cota-Arriola et al., 2011). However, low Mw CH exhibited only very modest inhibition activity against *A. flavus* (Gabriel et al., 2015). The inhibition for *A. niger* was reported to be triggered mainly by the electrostatic interactions affecting the spores and the germ tube emergence (Plascencia-Jatomea et al., 2003) and the spore germination rate (Cota-Arriola et al., 2011). Our results clearly show that hydrophobic interactions are very important for the antifungal activity and the insertion of dodecyl groups, i.e., imparting an increased amphipathic nature to the polymer backbone was responsible for the improved activity against *A. flavus* (Rabea, Badawy, Steurbaut, & Stevens, 2009). Bearing in mind that hydrophobic interactions play an important role in the inhibition of *A. flavus* and that this activity can be triggered by interaction with the wall and membrane of the fungus, subsequent steps in the present study were directed to the investigation of possible mechanisms involved in the inhibition.

### 3.3. Interaction of the amphiphilics with model membranes

The antifungal mode of action of chitosan on different fungi types has been widely studied (Goy, Britto, & Assis, 2009) and the electrostatic and hydrophobic interactions with negatively charged cell membranes have also been recognized as important components of its antifungal activity (Palma-Guerrero et al., 2010). Hence, and taking into account that chitosan molecules may diffuse through spores and reach the cell membrane (Li et al., 2011; Palma-Guerrero et al., 2010), the investigation of these interactions with PC and anionic PC:PG (80:20) model membranes and the role of Mw on them, may bring new insights to the antifungal activity investigation. Although these are simple mimetic systems of fungal membranes, they exemplify their high zwitterionic and low anionic characteristics (Dennison et al., 2014; Löffler et al., 2000; Lohner & Prenner, 1999; Lösel, 1990; Palma-Guerrero et al., 2010; Yeaman & Yount, 2003). The interaction of chitosan and derivatives with liposomes was evaluated by measurements of size and zeta potential of mixtures prepared at increasing polymer concentrations. Overall, the interaction was influenced by the presence of hydrophobic groups, Mw and the vesicle surface charge.

The addition of small amounts of CH130 to PC and PC:PG liposome solutions resulted in abrupt increases on measured average sizes (Fig. 3a and b), inducing the formation of micrometric aggregates at polymer concentrations as low as 0.01 g/L. This profile of size variation was more abrupt in the presence of the negatively charged PC:PG membranes, causing a rapid charge inversion with the formation of positively charged aggregates of +20 mV zeta potential, while for PC vesicles, zeta potential reached +10 mV at 1.0 g $L^{-1}$ of added polymer. Above certain concentrations, average hydrodynamic diameter (Dh) decreased denoting an aggregation/disaggregation process that correlated well with the zeta potential values. This trend was also observed for the interaction of the non-dodecylated derivative DEAE- $CH_{130}$ with PC vesicles (Fig. 3c). However, Dhs of PC vesicles, initially 100 nm in size, increased only gradually in the presence of DEAE- $CH_{130}$, and at the highest polymer concentration of 1.0 g $L^{-1}$ reached 200 nm. Moreover, zeta potential of the mixtures of DEAE-$CH_{130}$ with PC vesicles reached higher zeta values (+20 mV), indicating a more efficient adsorption on the liposome surface. Accordingly, the aggregation process decreased due to electrostatic repulsion between the charged liposomes as reported in earlier studies (Quemeneur, Rinaudo, & Pépin-Donat, 2008; Tan, Feng, Zhang, Xia, & Xia, 2016). The more efficient adsorption of DEAE-$CH_{130}$ compared to CH can be explained taking into account its more hydrophobic character inferred from the fluorescence studies with pyrene. Hence, its tendency to self-assemble in solution and its more amphipathic character may favor stronger interactions with the model membranes, conferring increased positive zeta potential to the liposomes.

This trend was also observed with the hydrophobically modified DEAE derivatives (Fig. 3e–j). However, the strength of interaction with PC and PC:PG liposomes was reinforced by the presence of dodecyl groups and showed a clear dependence on the Mw and the surface charge of the liposomes. The insertion of dodecyl groups into DEAE-CH derivatives provided stronger interactions with PC and PC:PG liposomes and the addition of aliquots as low as $5.0 \times 10^{-3}$ g.$L^{-1}$ induced more abrupt changes on the measured sizes, indicating the formation of larger aggregates. Moreover, the higher Mw derivatives (DEAE¬$CH_{70}$-Dod, and DEAE¬$CH_{130}$-Dod) induced more sudden changes to PC and PC:PG vesicle sizes. Besides electrostatic forces, the interaction of

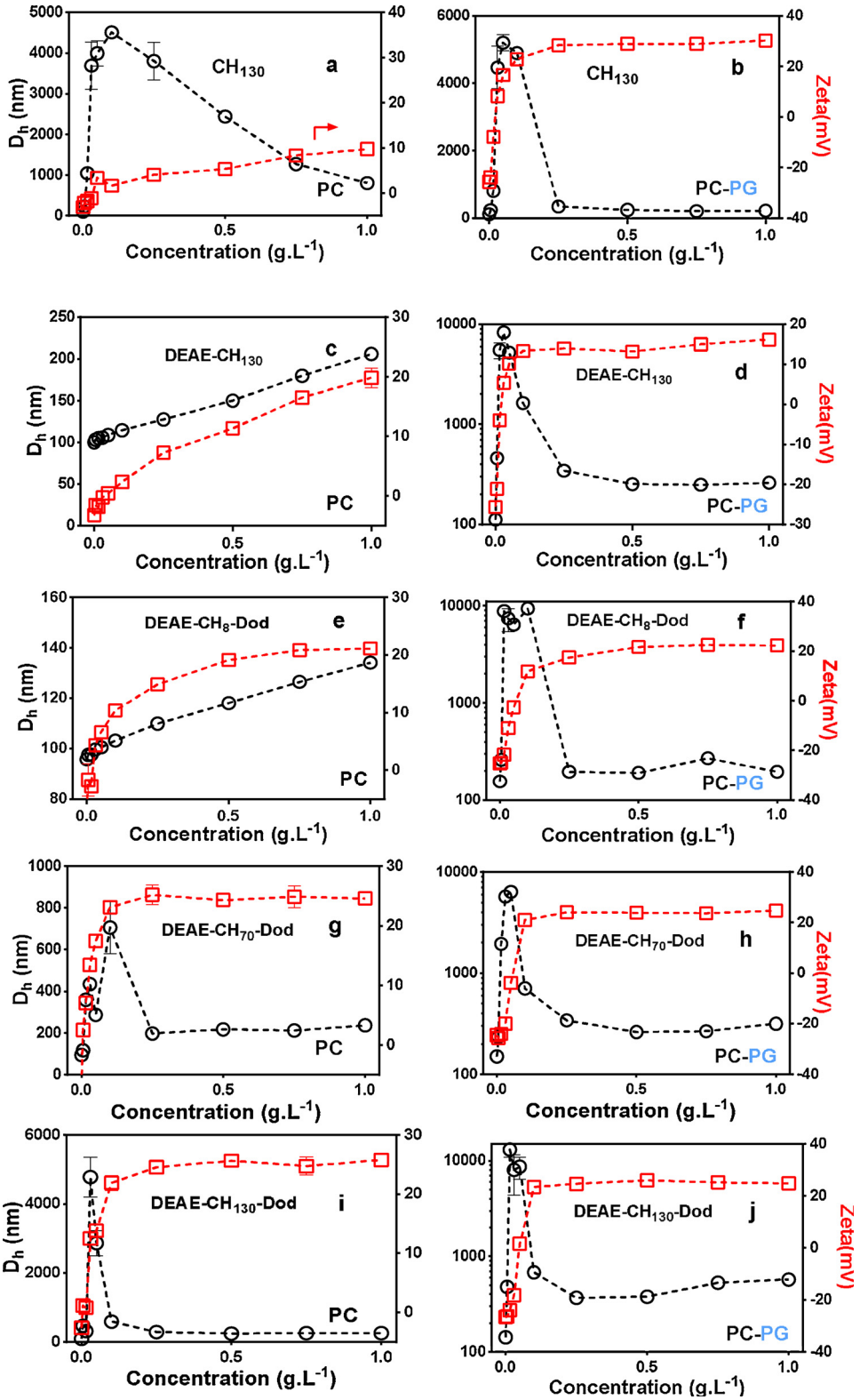


**Fig. 3.** Comparative measurements of size (black circles) and zeta potential (red squares) for PC and PC:PG model membranes in the presence of increasing concentrations of $CH_{130}$, DEAE-$CH_{130}$ and the dodecylated derivatives of DEAE¬CH-Dod of 8, 70 and 130 kDa. Error bars correspond to the s.d. of triplicate measurements of the same sample; when not visible it means it is smaller than the symbol. (For interpretation of the references to colour in this figure legend, the reader is referred to the web version of this article.)

amphiphilic chitosans with phospholipid vesicles has been reported to be driven by the intercalation of hydrophobic groups into the lipid bilayers (Tiera, Tiera, & Winnik, 2010). Hence, the stronger aggregation provided by the amphiphilics of higher Mw may be explained taking into account that longer polymer chains offer more hydrophobic groups for insertion into the model membranes.

The importance of membrane surface charge for the liposome-amphiphilic interaction is more clearly seen by comparing zeta potential

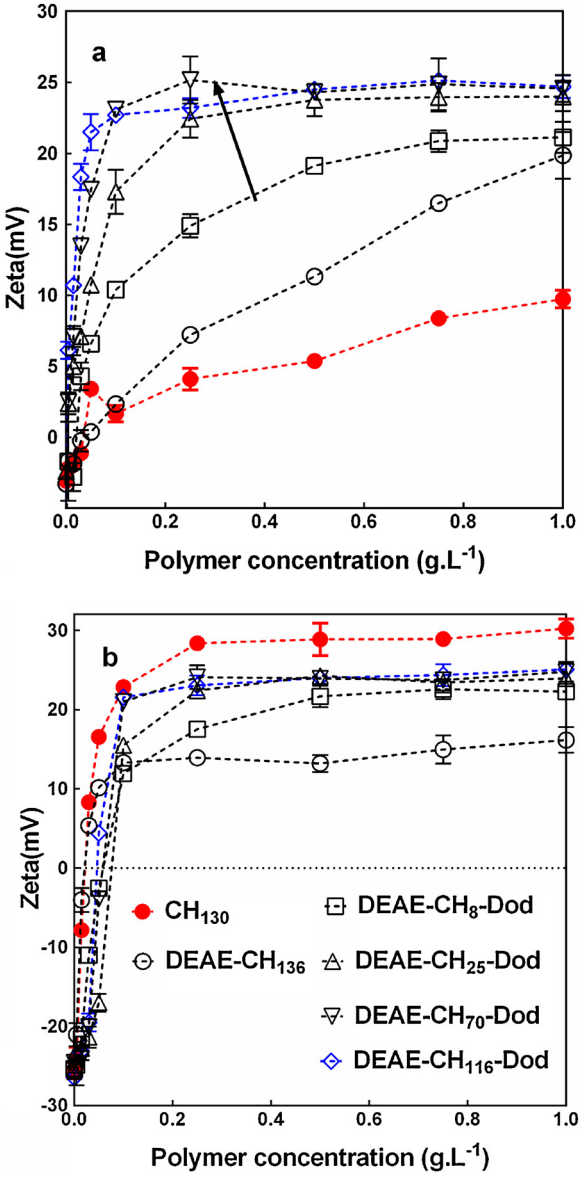


**Fig. 4.** Zeta potential of (a) PC and (b) PC:PG vesicles as a function of polymer concentration. The arrow indicates an improved adsorption with the increase of Mw (8–136 kDa). Red filled circles refer to deacetylated chitosan and blue empty diamonds to the amphiphilic chitosan derivatives of higher Mw, DEAE-$CH_{130}$-Dod. (For interpretation of the references to colour in this figure legend, the reader is referred to the web version of this article.)

values of all mixtures in the presence of PC and PC:PG vesicles (Fig. 4a and b). The zeta potential of PC vesicles becomes increasingly positive with the polymer concentration. However, each polymer displays a different increase and the amphiphilic derivatives of higher Mw were more strongly adsorbed to the vesicles surface. The negatively charged membrane of PC:PG vesicles induced stronger interactions with $CH_{130}$ and, compared to the amphiphilic chitosan derivatives, a more sudden charge inversion took place, producing decorated liposomes with more positive zeta potential values of +28 mV and zeta potential variation, Δzeta, above +40 mV (Fig. 4b). Although the addition of the amphiphilic chitosan derivatives to PC:PG suspension had also resulted in a steep increase in zeta potential, the final values remained around +22 mV. This difference can be explained taking into account that the chains of $CH_{130}$ remain free in the bulk and accordingly, available for the adsorption process, while for the amphiphilics, the availability of free chains is diminished by the concurrent self-aggregation process. It can also be speculated that, for $CH_{130}$, a more extended polymer chain is expected that would favor its bending and adsorption on the vesicular surface (Mertins & Dimova, 2011), whereas for the amphiphilic chitosan derivatives, the intramolecular hydrophobic forces may lead to more coiled conformations restraining the adsorption onto the vesicles. Fig. 4b shows the effect of Mw on the adsorption process, where slightly more positive zeta potential values are produced by higher Mw derivatives (DEAE-$CH_{116}$-Dod and DEAE-$CH_{70}$-Dod).

As previously reported, the adsorption of chitosan onto phospholipid vesicles is driven mainly by electrostatic interaction and it is reinforced by the presence of negatively charged phospholipids (Quemeneur et al., 2008). Alterations of and damage to cell membranes of fungi with chitosans of low Mw against *Candida* species (Kulikov et al., 2014) and *Neurospora crassa* (Palma-Guerrero et al., 2009) have been reported. On the other hand, a fungistatic mechanism has been proposed for *Aspergillus parasiticus* and attributed to the high Mw (170–300 kDa) of the chitosan samples used (Seyfarth, Schliemann, Elsner, & Hipler, 2008). Results shown here confirm that a combination of grafting with DEAE, hydrophobic groups and a precise control of Mw is a promising way to achieve stronger interactions with the cell membrane.

To evaluate the ability of these amphiphilic chitosan derivatives of permeabilizing the model membranes, the interaction was studied using CF-loaded vesicles (CF-PC:PG, Fig. 5). In general, no leaking was observed for the amphiphilics tested and a comparative experiment is shown in Fig. 5a. It can be noticed that, after addition of the amphiphilic DEAE-$CH_8$–Dod (cuvette B at the center of the picture), the solution becomes slightly cloudy due to aggregation. However, no visible sign of the characteristic yellowish-green color of diluted CF can be seen. The fluorescence of CF-loaded PC:PG vesicles was monitored in the presence of increasing concentrations of DEAE¬$CH_8$–Dod and DEAE¬$CH_{130}$–Dod and these are shown in Fig. 5b and c, respectively. As can be seen from these figures, the addition of both amphiphilics in the range of 0.03–1.0 g/L did not produce any increase in the fluorescence intensity. In addition, the aggregation induced by the polycations increases the scattered light, decreasing the intensity and supporting a mechanism of adsorption of polymer chains on the negatively charged vesicular surface (Fig. 5b and c, pink bars). Moreover, this result indicates that, in this concentration range, the integrity of the lipid bilayer is not compromised, since for all three tested concentrations, no fluorescence increase was observed.

The PC:PG coated vesicles were subsequently challenged by adding TRITON-X100 to induce the disruption of the bilayer. For the lower polymer concentrations of 0.03 g $L^{-1}$ and 0.25 g $L^{-1}$, the coating is partial and the fluorescence intensity increased because of CF leaking (Fig. 5a and b, green bars). Further addition of polymer, at the concentration of 1 g $L^{-1}$, produced the charge reversion and a more complete coating of the vesicular surface. Hence, the addition of TRITON-X100 resulted only in minor increases in fluorescence, corroborating the interpretation given to DLS and zeta potential measurements (Fig. 3) and supporting the proposal of formation of stabilized liposomes (Quemeneur, Rinaudo, Maret, & Pépin-Donat, 2010; Tan et al., 2015, 2016). However, the formation of pores cannot be disregarded by the present results, being dependent on the type of liposome (Mertins & Dimova, 2013) and the concentration used in the experiment (Tan et al., 2015).

Overall, it can be concluded that the presence of hydrophobic groups in the polymer backbone may give place to polymer-polymer, polymer-cell wall and polymer-cell membrane interactions. The inhibition assay showed that the decrease in molecular weight resulted in an increased antimicrobial activity, revealing that Mw is an important factor and its increase strengthens the intermolecular polymer-polymer hydrophobic forces. This interpretation is supported by the lower CAC values (Table 1) and indicates that self-aggregation of the higher molar mass amphiphilic derivatives limits their antimicrobial activity, indicating a concurrence between the self-aggregation and the interaction

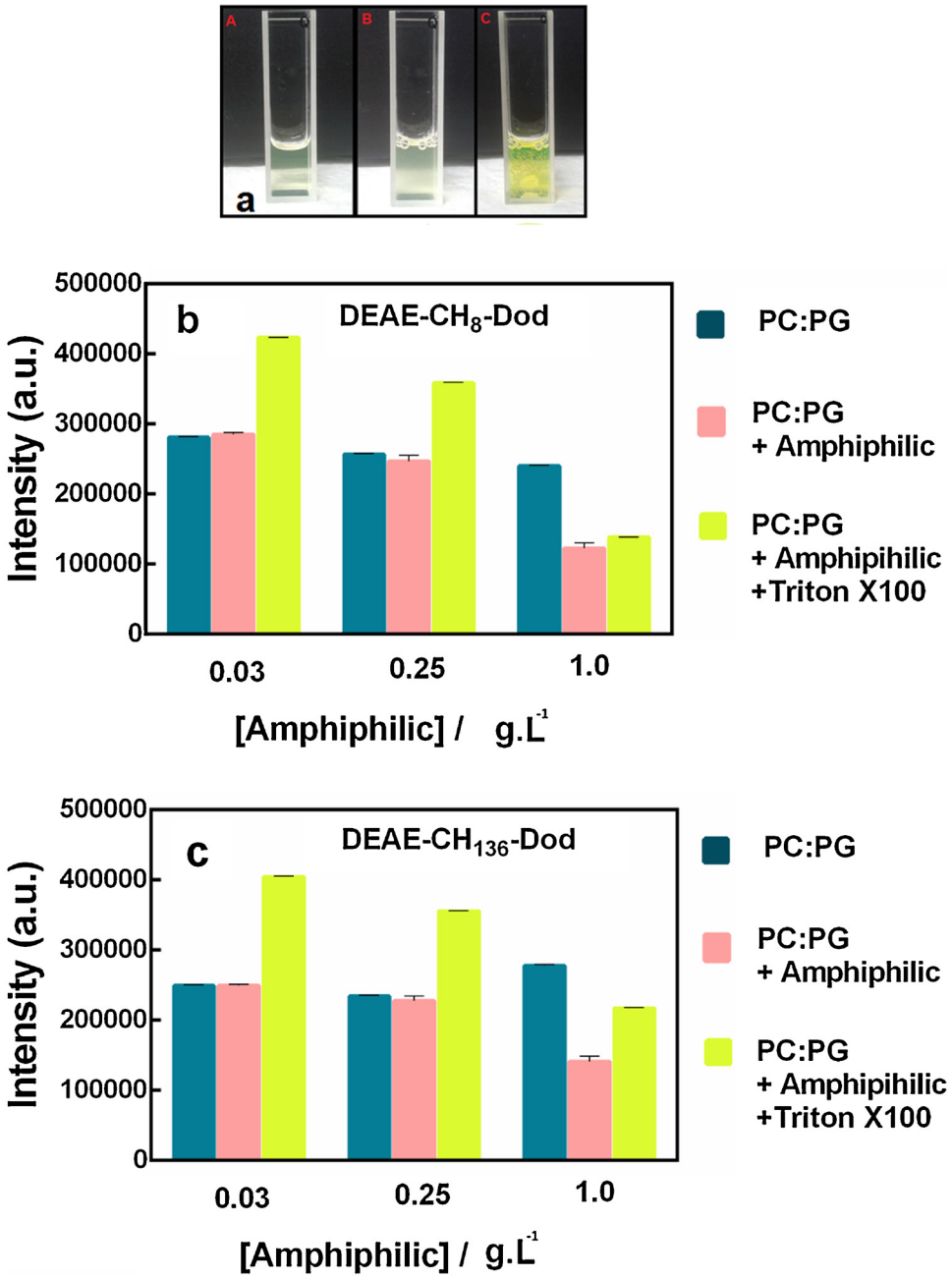


**Fig. 5.** a) Experiment of dye leakage of entrapped CF from PC:PG LUVs in the absence of polymer: cuvette A (negative control); cuvette B, after addition of 1.0 g $L^{-1}$ of DEAE¬$CH_8$–Dod; and cuvette C, after addition of Triton X-100, positive control. Fluorescence intensity of CF-loaded PC:PG vesicles as a function of b) DEAE¬$CH_8$ −Dod and c) DEAE¬$CH_{136}$ −Dod concentration.

with the fungal structures.

The results from the study with PC and PC:PG membranes clearly suggest that besides hydrophobic interactions, the electrostatic interactions originating from the presence of negatively charged lipids increases the adsorption to the membrane surface. As previously reported, anionic lipids are also found in the composition of the fungal membrane of *A. flavus,* mainly phosphatidylinositol, at about 15% (Dennison et al., 2014). Hence, increased adsorption of the amphiphilic derivatives on the membranes is driven by the negative lipids of *A. flavus* and supports the higher antifungal activity of the lower Mw derivatives DEAE-$CH_8$-Dod and DEAE-$CH_{25}$-Dod, which exhibit weaker polymer-polymer self-associations. In support of this interpretation, a similar result was reported for amphiphilic quaternary oligomeric chitosan derivatives, whose antibacterial activities were higher than those obtained with the higher MW chitosan polymer (Rúnarsson et al., 2010). Moreover, the stronger hydrophobic and electrostatic interactions with the cell membrane may potentialize the stress responses of the fungus. As demonstrated for other fungi types, such as *Ustilago maydis* (Olicón-Hernández, Uribe-Alvarez, Uribe-Carvajal, Pardo, & Guerra-Sánchez, 2017), *R. stolonifera* (Alfaro-Gutiérrez, Guerra-Sánchez, Hernández-Lauzardo, & Velázquez-del Valle, 2014), *Candida albicans* (Pena, Sanchez, & Calahorra, 2013) and *Neurospora crassa* (Lopez-Moya et al., 2016), the permeabilization of the cell membrane, triggers the oxidative stress. Hence, as indicated by our study, the higher ability of our amphiphilic derivatives of binding to the cell membrane cannot be neglected and contributes to the inhibition of the fungal growth.

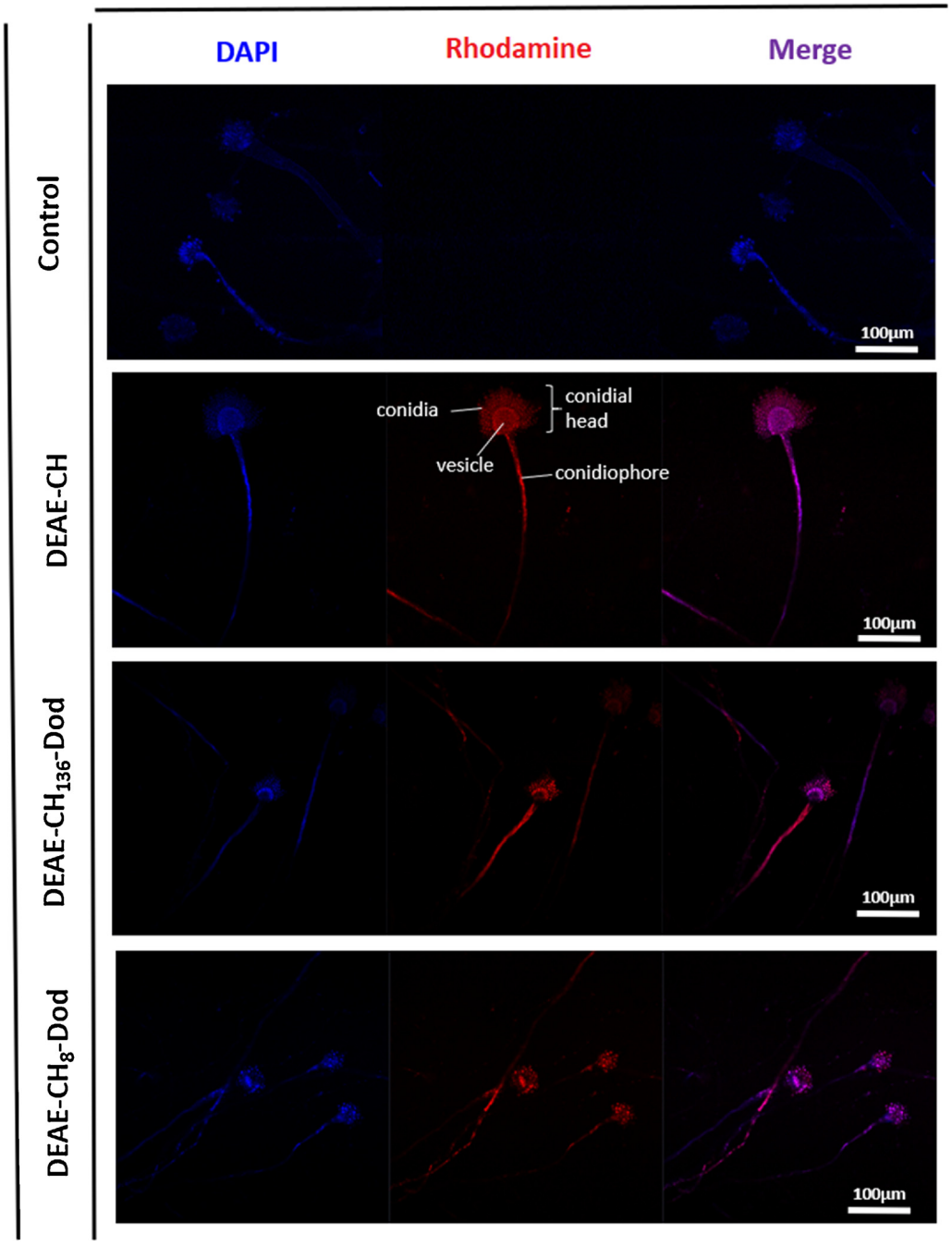


**Fig. 6.** Laser confocal scanning microscopy of *A. flavus* grown in PDA labeled with DAPI (Control), exhibiting preserved conidiophore, vesicle and conidia, and the fungus treated with DEAE-CH and its dodecylated derivatives of higher and lower molecular weight, DEAE-$CH_{136}$-Dod and DEAE-$CH_8$-Dod, respectively, displaying distorted conidiophore, shrunken vesicles, and a decreased population of conidia (DEAE-$CH_8$-Dod). Magnification: 1200×.

### *3.4. Interaction of amphiphilic derivatives and the fungus monitored by laser confocal scanning microscopy and electronic transmission microscopy*

The interactions between the amphiphilic derivatives and the cell wall and the cell membrane were investigated by confocal microscopy. The rhodamine-labeled derivatives were incubated with *A. flavus* to evaluate the ability of the amphiphilic compounds to adhere to the fungal structures. Fig. 6 shows the images obtained from non-treated fungus, the hydrophilic chitosan derivative DEAE-CH and its derivatives of higher and lower Mw (DEAE-$CH_{136}$-Dod and DEAE-$CH_8$-Dod). The images show that chitosan and all tested amphiphilics strongly adhered to the hyphae, phialides and conidiophores. The fungus treated with DEAE-CH showed preserved structures with no visible alterations of the morphology, similar to the non-treated fungus (Fig. 6, control). Confocal images also show that the fungus growth in the presence of DEAE-$CH_8$-Dod or DEAE-$CH_{136}$-Dod exhibited alterations and distortions on the conidiophore, shrunken vesicles and a decreased conidiophore population.

More details regarding the consequences of these interactions on the conidia were obtained from TEM. Fig. 7a–c show the conidia of non-treated fungus, which exhibited a preserved cell wall (CW) structure with a uniform distribution of layer constituents surrounding the cell membrane. On the other hand, *A. flavus* treated with DEAE-CH (Fig. 7d and e) exhibit some regions in which the structure is preserved but also some areas where an aggregated phase is visible denoted by small black spots. These small aggregates are more easily observed for the fungus

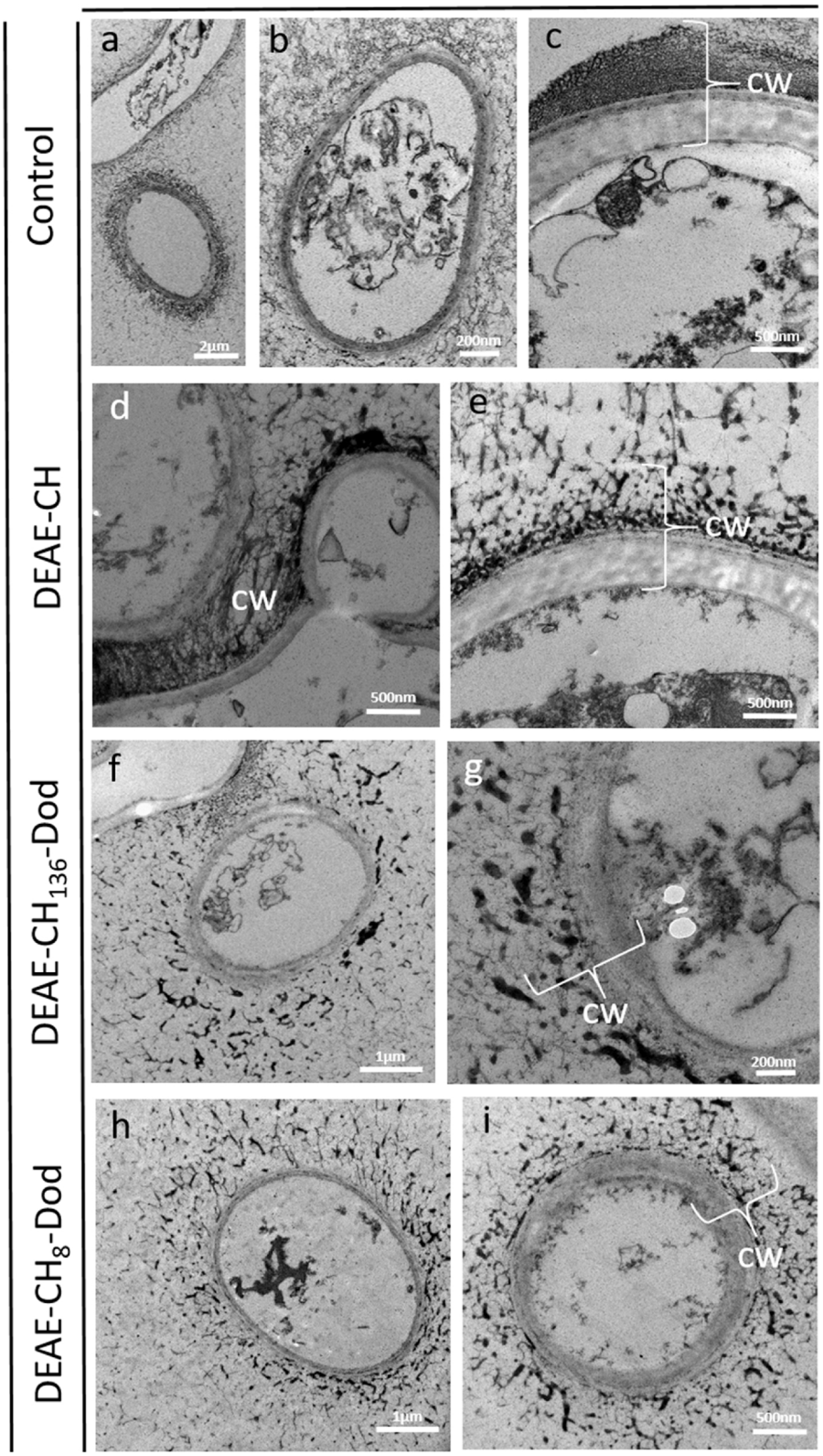


**Fig. 7.** Scanning electron micrographs of *A. flavus* grown on PDA nutrient agar. (a, b and c) In the absence of polymer showing well-defined conidia with a preserved cell structure. (d and e) In the presence of DEAE-CH with partial aggregation of the cell wall. (f, g) In the presence of DEAE-$CH_{136}$-Dod and (h, i) in the presence of DEAE-$CH_8$-Dod. The final four images (f–i) exhibit an extensive aggregation of the cell wall constituents. Magnification Figures: (a): 5000×, (b, g): 50000×, (c, d, e, i): 75000×, (f, h): 2500×.

treated with DEAE-$CH_{136}$-Dod (Fig. 7f and g) and DEAE-$CH_8$ -Dod (Fig. 7h and i). Similar ultrastructural alterations had been observed in an earlier study on the interaction of chitosan derivatives with *Saprolegnia parasitica*, in which the cell wall was observed either thinner or thicker than normal and the membrane was only partially visible (Muzzarelli et al., 2001).

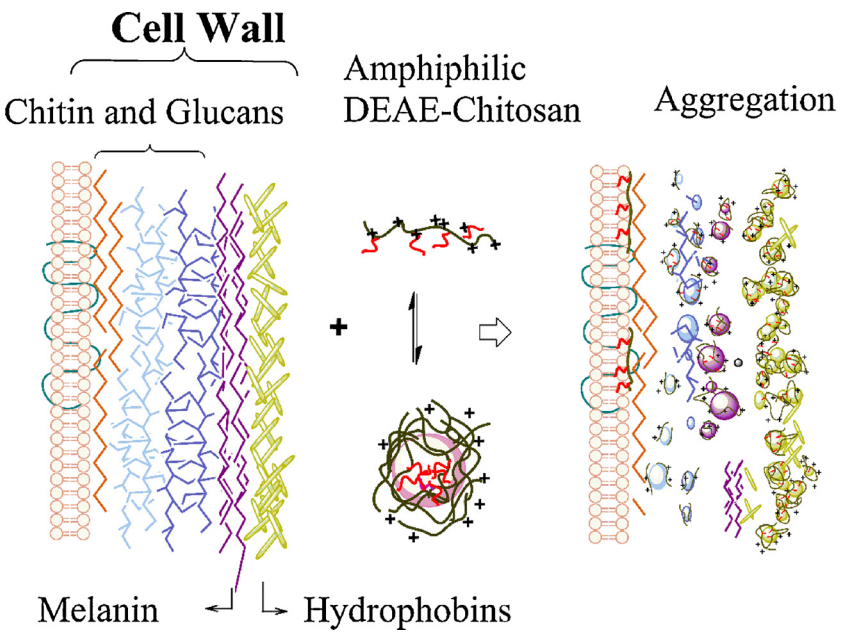


**Fig. 8.** Schematic representation of the adsorption of amphiphilic DEAE-chitosan on cell wall and cell membrane of *A. flavus* resulting from interactions with their chains and aggregates. Hydrohobins and melanin are more prone to aggregation due to their amphiphilic character and anionic charges. Amphiphilic chains of lower Mw can also interact with the cell membrane affecting its permeability.

It is well known that the cell wall is a vital structure for fungi, especially for protection against dehydration and against changes in osmotic pressure and attack of pathogens. In particular, hyphae have hydrophobic proteins and the surface of conidia reported to have a layer of "rodlets". One of the suggested functions of rodlets is to act as a water repellent, with structures known as "hydrophobins" that have a hydrophobic and a hydrophilic part (Erwig & Gow, 2016; Littlejohn, Hooley, & Cox, 2012). Our results indicate that the amphiphilic nature of the chitosan derivatives favors the electrostatic targeting of hydrophilic components and strong interactions with the hydrophobic rodlets present in the cell wall (Fig. 8). Moreover, melanins are hydrophobic pigments polymerized from phenolic or indolic compounds that have high molecular weight, negative charge and are also present on the wall of the conidia (Erwig & Gow, 2016). Therefore, the aggregates appearing in the images may result from hydrophobic and electrostatic interactions with the conidia pigments. Altogether these effects contribute to the breakdown of the defense barrier allowing the access of amphiphilic chitosans to the cell membranes. Hence, after binding to the conidial surface, the amphiphilics might affect the morphogenetic events responsible for growth and germination. Additionally, the lower Mw derivatives may more easily cross the cell wall, reaching the plasma cell membrane of the fungus, which in turn may affect the membrane permeability properties (Palma-Guerrero, Jansson, Salinas, & Lopez-Llorca, 2008), triggering other mechanisms such as membrane function impairment.

## 4. Conclusions

Amphiphilic derivatives of chitosan of varied molecular weights and with fixed contents of tertiary amino groups and hydrophobic grafts were successfully synthesized. The *in vitro* assay showed that hydrophobic groups have a central role in the antifungal activity of these amphiphilics and that the decreasing Mw was pivotal to achieving higher inhibition of the fungal growth. Moreover, our results show that polymer-polymer and polymer-fungus interactions are concurrent and that, by increasing Mw, polymer-polymer interactions were favored, decreasing the antifungal activity. The study of the interaction with model membranes showed that these amphiphilics strongly partition to the cell membrane surface. This adsorption is greatly reinforced by the presence of negatively charged lipids, which are also found in the composition of the fungal membrane of *Aspergillus flavus*. Considering that, for the lower molecular weight chitosan amphiphilics, the polymer-polymer interactions are weaker, they were more likely to interact with cell wall constituents. Further investigation using CLSM demonstrated the strong interaction of the polycations with the conidiophores and conidial head, directly affecting the sporulation phase. The aggregation of constituents of the cell wall, which were induced by the amphiphilic derivatives, was shown by transmission electronic microscopy and indicates that the integrity of the cell wall is affected.

## Acknowledgements

This work was supported by the Fundação de Amparo à Pesquisa do Estado de São Paulo, Brazil (Grant 2016/15736-0). The Authors wish to thank Dr. Odílio Benedito Garrido Assis, Embrapa Instrumentação Agropecuária, São Carlos for access to instrumentation. A. M. F. Lima acknowledges the support of CAPES (Grant PNPD 1267244) for her postdoctoral scholarship. M.P.D.S.C. acknowledges FAPESP support 2014/08372-7.

## Appendix A. Supplementary data

Supplementary data associated with this article can be found, in the online version, at https://doi.org/10.1016/j.carbpol.2018.05.032.

## References

Alfaro-Gutiérrez, I. C., Guerra-Sánchez, M. G., Hernández-Lauzardo, A. N., & Velázquez-del Valle, M. G. (2014). Morphological and physiological changes on *rhizopus stolonifer* by effect of chitosan, oligochitosan or essential oils. *Journal of Phytopathology, 162*, 723–730.

Alkan, D., & Yemenicioglu, A. (2016). Potential application of natural phenolic antimicrobials and edible film technology against bacterial plant pathogens. *Food Hydrocolloids, 55*, 1–10.

Bonilla, J., & Sobral, P. J. A. (2016). Investigation of the physicochemical, antimicrobial and antioxidant properties of gelatin-chitosan edible film mixed with plant ethanolic extracts. *Food Bioscience, 16*, 17–25.

Cabrera, M. P. S., Costa, S. T., de Souza, B. M., Palma, M. S., Ruggiero, J. R., & Ruggiero Neto, J. (2008). Selectivity in the mechanism of action of antimicrobial mastoparan peptide Polybia-MP1. *European Biophysics Journal, 37*, 879–891.

Casé, A. H., Picola, I. P. D., Zaniquelli, M. E. D., Fernandes, J. C., Winnik, F. M., & Tiera, M. J. (2009). Physicochemical characterization of nanoparticles formed between DNA and phosphorylcholine substituted chitosans. *Journal of Colloid and Interface Science, 336*(1), 125–133.

Chang, P. K., & Ehrlich, K. C. (2010). Review: What does genetic diversity of Aspergillus flavus tell us about Aspergillus oryzae? *International Journal of Food Microbiology, 138*(3), 189–199 201.

Cota-Arriola, O., Cortez-Rocha, M. O., Rosas-Burgos, E. C., Burgos-Hernandez, A., Lopez-Franco, Y. L., & Plascencia-Jatomea, M. (2011). Antifungal effect of chitosan on the

growth of Aspergillus parasiticus and production of aflatoxin B1. *Polymer International, 60*, 937–944.
Cotta-Pereira, G., Guerra, R. F., & Bittencourt-Sampaio, S. (1976). Oxytalan, eulaunin and elastic fibers in the human skin. *J. Invest. Dermatol. 66*, 143–148.
DAPI (2018). *Protocol for fluorescence imaging. (2018, May 5).* Retrieved from https://www.thermofisher.com/br/pt/home/references/protocols/cell-and-tissue-analysis/protocols/dapi-imaging-protocol.html.
De Oliveira, V. A., Tiera, M. J., & Neumann, M. G. (1996). Interaction of cationic surfactants with acrylic acid-ethyl methacrylate copolymers. *Langmuir, 12*(3), 607–612.
De, A., Borse, R., Kumar, A., & Mozundar, S. (2014). *Targeted delivery of pesticide using biodegradable polymeric nanoparticles* (1rst ed.). New York: Springer.
Dennison, S. R., Morton, L. H. G., Harris, F., & Phoenix, D. A. (2014). The interaction of aurein 2.5 with fungal membranes. *European Biophysical Journal, 43*, 255–264.
Desbrieres, J., Martinez, C., & Rinaudo, M. (1996). Hydrophobic derivatives of chitosan: Characterization and rheological behaviour. *International Journal of Biological Macromolecules, 19*, 21–28.
Erwig, L. P., & Gow, N. A. R. (2016). Interactions of fungal pathogens with phagocytes. *Nature Reviews Microbiology, 14*(3), 163–176.
Fakruddin, M., Chowdhury, A., Hossain, M. N., & Ahmed, M. M. (2015). *Characterization of aflatoxin producing Aspergillus flavus from food and feed samples*, *Vol. 4*, SpringerPlus159.
Gabriel, J. S., Tiera, M. J., & Tiera, V. A. O. (2015). Synthesis, characterization and antifungal activity of amphiphilic derivatives of diethylaminoethyl-chitosan against Aspergillus flavus. *Journal of Agricultural and Food Chemistry, 63*(24), 5725–5731.
Goy, R. C., Britto, D., & Assis, O. B. G. (2009). A review of the antimicrobial activity of chitosan. *Polímeros: Ciência E Tecnologia, 19*(3), 241–247.
Hedayati, M. T., Pasqualotto, A. C., Warn, P. A., Bowyer, P., & Denning, D. W. (2007). Aspergillus flavus: Human pathogen, allergen and mycotoxin producer. *Microbiology, 153*, 1677–1692.
Huang, R., Du, Y., Zheng, L., Liu, H., & Fan, L. (2004). A new approach to chemically modified chitosan sulfates and study of their influences on the inhibition of Escherichia coli and Staphylococcus aureus growth. *Reactive & Functional Polymers, 59*, 41–51.
Huang, M., Khor, E., & Lim, L. (2004). Uptake and cytotoxicity of chitosan molecules and nanoparticles: Effects of molecular weight and degree of deacetylation. *Pharmaceutical Research, 21*(2), 344–353.
Ignatova, M., Starbova, K., Markova, N., Manolovaa, N., & Rashkov, I. (2006). Electrospun nano-fibre mats with antibacterial properties from quaternised chitosan and poly (vinyl alcohol). *Carbohydrate Research, 341*, 2098–2107.
Kong, M., Chen, X. G., Xing, K., & Park, H. J. (2010). Antimicrobial properties of chitosan and mode of action: A state of the art review. *International Journal of Food Microbiology, 144*, 51–63.
Kulikov, S. N., Lisovskaya, S. A., Zelenikhin, P. V., Bezrodnykh, E. A., Shakirova, D. R., Blagodatskikh, I. V., & Tikhonov, V. E. (2014). Antifungal activity of oligochitosans (short chain chitosans) against some Candida species and clinical isolates of Candida albicans: Molecular weight-activity relationship. *European Journal of Medicinal Chemistry, 74*(3), 169–178.
Löffler, J., Einsele, H., Hebart, H., Schumacher, U., Hrastnik, C., & Daum, G. (2000). Phospholipid and sterol analysis of plasma membranes of azole-resistant Candida albicans strains. *Microbiology Letters, 185*, 59–63.
Lösel, D. M., et al. (1990). Lipids in the structure and function of fungal membranes. Biochemistry of cell walls and membranes. In P. J. Kuhn (Ed.). *Fungi* (pp. 119–133). Berlin Heidelberg: Springer-Verlag.
Lacerda, A. F., Vasconcelos, E. A. R., Pelegrini, P. B., & de Sa, M. F. G. (2014). Antifungal defensins and their role in plant defense. *Frontiers in Microbiology, 5*, 116.
Li, M., Chen, X., Liu, J., Zhang, W., & Tang, X. (2011). Molecular weight-dependent antifungal activity and action mode of chitosan against *Fulvia fulva*(Cooke) Ciffrri. *Journal of Applied Polymer Science, 119*, 3127–3135.
Littlejohn, K. A., Hooley, P., & Cox, P. W. (2012). Bioinformatics predicts diverse Aspergillus hydrophobins with novel properties. *Food Hydrocolloids, 27*(2), 503–516.
Lohner, K., & Prenner, E. J. (1999). Differential scanning calorimetry and X-ray diffraction studies of the specificity of the interaction of antimicrobial peptides with membrane-mimetic systems. *Biochimica Et Biophysica Acta, 1462*(1–2), 141–156.
Lopez-Moya, F., Kowbel, D., Nueda, M. J., Palma-Guerrero, J., Glass, N. L., & Lopez-Llorca, L. V. (2016). Neurospora crassa transcriptomics reveals oxidative stress and plasma membrane homeostasis biology genes as key targets in response to chitosan. *Molecular Biosystems, 12*(2), 391–403.
Mertins, O., & Dimova, R. (2011). Binding of chitosan to phospholipid vesicles studied with isothermal titration calorimetry. *Langmuir, 27*(9), 5506–5515.
Mertins, O., & Dimova, R. (2013). Insights on the interactions of chitosan with phospholipid vesicles: Part II: Membrane stiffening and pore formation. *Langmuir, 29*(47), 14552–14559.
Mortensen, K. L., Mellado, E., Lass-Florl, C., Rodriguez-Tudela, J. L., Johansen, H. K., & Arendrup, M. C. (2010). Environmental study of azole-resistant Aspergillus fumigatus and other aspergilli in Austria, Denmark, and Spain. *Antimicrobial Agents and Chemotherapy, 54*, 4545–4549.
Muzzarelli, R. A. A., Muzzarelli, C., Tarsi, R., Miliani, M., Gabbanelli, F., & Cartolari, M. (2001). Fungistatic activity of modified chitosans against Saprolegnia parasítica. *Biomacromolecules, 2*, 165–169.
Nogueira, J. H. C., Gonçalez, E., Galleti, S. R., Facanali, R., Marques, M. O., & Felício, J. D. (2010). Ageratum conyzoides essential oil as aflatoxin suppressor of Aspergillus flavus. *International Journal of Food Microbiology, 137*, 55–60.
Olicón-Hernández, D. R., Uribe-Alvarez, C., Uribe-Carvajal, S., Pardo, J. P., & Guerra-Sánchez, G. (2017). Response of *Ustilago maydis* against the stress caused by three polycationic chitin derivatives. *Molecules, 22*(12), 1745. http://dx.doi.org/10.3390/molecules22121745.
Palma-Guerrero, J., Jansson, H.-B., Salinas, J., & Lopez-Llorca, L. V. (2008). Effect of chitosan on hyphal growth and spore germination of plant pathogenic and biocontrol fungi. *Journal of Applied Microbiology, 104*, 541–553.
Palma-Guerrero, J., Huang, I.-C., Jansson, H.-B., Salinas, J., Lopez-Llorca, L. V., & Read, N. D. (2009). Chitosan permeabilizes the plasma membrane and kills cells of Neurospora crassa in an energy dependent manner. *Fungal Genetics and Biology, 46*, 585–594.
Palma-Guerrero, J., Lopez-Jimenez, J. A., Pérez-Berná, A. J., Huang, I.-C., Jansson, H.-B., Salinas, J., Villalaín, J., Read, N. D., & Lopez-Llorca, L. V. (2010). Membrane fluidity determines sensitivity of filamentous fungi to chitosan. *Molecular Microbiology, 75*(4), 1021–1032.
Park, D. L., & Troxell, T. C. (2002). U.S. perspective on mycotoxin regulatory issues. *Advances in Experimental Medicine and Biology, 504*, 227–285.
Pedro, R. O., Takaki, M., Gorayeb, T. C. C., Thomeo, J. C., Del Bianchi, V. L., Tiera, M. J., & Tiera, V. A. O. (2013). Synthesis, characterization and antifungal activity of quaternary derivatives of chitosan on *Aspergillus flavus*. *Microbiological Research, 168*, 50–55.
Pena, A., Sanchez, N. S., & Calahorra, M. (2013). Effects of chitosan on Candida albicans: Conditions for its antifungal activity. *BioMed Research International, 2013*. http://dx.doi.org/10.1155/2013/527549 Article ID 527549.
Plascencia-Jatomea, M., Viniegra, G., Olayo, R., Castillo-Ortega, M. M., & Shirai, K. (2003). Effect of chitosan and temperature on spore germination of Aspergillus niger. *Macromolecular Bioscience, 3*(10), 582–586.
Quemeneur, F., Rinaudo, M., & Pépin-Donat, B. (2008). Influence of molecular weight and pH on adsorption of chitosan at the surface of large and giant vesicles. *Biomacromolecules, 9*(1), 396–402.
Quemeneur, F., Rinaudo, M., Maret, G., & Pépin-Donat, B. (2010). Decoration of lipid vesicles by polyelectrolytes: Mechanism and structure. *Soft Matter, 6*, 4471–4481.
Rúnarsson, Ö. V., Holappa, J., Malainer, C., Steinsson, H., Hjálmarsdóttir, M., Nevalainen, T., & Másson, M. (2010). Antibacterial activity of N-quaternary chitosan derivatives: Synthesis, characterization and structure activity relationship (SAR) investigations. *European Polymer Journal, 46*, 1251–1267.
Rabea, E. I., Badawy, M. E. I., Steurbaut, W., & Stevens, C. V. (2009). In vitro assessment of N-(benzyl)chitosan derivatives against some plant pathogenic bacteria and fungi. *European Polymer Journal, 45*, 237–245.
Rouser, G., Fleischer, S., & Yamamoto, A. (1970). Two dimensional thin layer chromatographic separation of polar lipids and determination of phospholipids by phosphorus analysis of spots. *Lipids, 5*, 494–496.
Saggiorato, A. G., Gaio, I., Treichel, H., Oliveira, D., Cichoski, A. J., & Cansian, R. L. (2012). Antifungal activity of basil essential oil (ocimum basilicum L.): Evaluation in vitro and on an italian-type sausage surface. *Food Bioprocess Technology, 5*, 378–384.
Sahariah, P., & Másson, M. (2017). Antimicrobial chitosan and chitosan derivatives: A review of the structure–activity relationship. *Biomacromolecules, 18*, 3846–3868.
Sajomsang, W., Gonil, P., Saesoo, S., & Ovatlarnporn, C. (2012). Antifungal property of quaternized chitosan and its derivatives. *International Journal of Biological Macromolecules, 50*, 263–269.
Seyfarth, F., Schliemann, S., Elsner, P., & Hipler, U.-C. (2008). Antifungal effect of high- and low-molecular-weight chitosan hydrochloride, carboxymethyl chitosan, chitosan oligosaccharide and N-acetyl-d-glucosamine against Candida albicans, Candida krusei and Candida glabrata. *International Journal of Pharmaceutics, 353*, 139–148.
Souza, R. H. F. V., Takaki, M., Pedro, R. O., Gabriel, J. S., Tiera, M. J., & Tiera, V. A. O. (2013). Hydrophobic effect of amphiphilic derivatives of chitosan on the antifungal activity against Aspergillus flavus and Aspergillus parasiticus. *Molecules, 18*(4), 4437–4450.
Tømmeraas, K., Vårum, K., Christensen, B. E., & Smidsrød, O. (2001). Preparation and characterization of oligosaccharides produced by nitrous acid depolymerization of chitosan. *Carbohydrate Research, 333*, 137–144.
Tamera, T. M., Hassan, M. A., Omer, A. M., Valachová, K., Eldin, M. S. M., Collinse, M. N., & Soltés, L. (2017). Antibacterial and antioxidative activity of O-amine functionalized chitosan. *Carbohydrate Polymers, 169*, 441–445.
Tan, C., Zhang, Y., Abbas, S., Feng, B., Zhang, X., Xia, W., & Xia, S. (2015). Biopolymer-lipid bilayer interaction modulates the physical properties of liposomes: Mechanism and structure. *Journal of Agricultural and Food Chemistry, 63*, 7277–7285.
Tan, C., Feng, B., Zhang, X., Xia, W., & Xia, S. (2016). Biopolymer-coated liposomes by electrostatic adsorption of chitosan (chitosomes) as novel delivery systems for carotenoids. *Food Hydrocolloids, 52*, 774–784.
Tayel, A. A., Moussa, S., El-Tras, W. F., Knittel, D., Opwis, K., & Schollmeyer, E. (2010). Anticandidal action of fungal chitosan against Candida albicans. *International Journal of Biological Macromolecules, 47*, 454–457.
Tiera, M. J., Qiu, X. P., Bechaouch, S., Shi, Q., Fernandes, J. C., & Winnik, F. M. (2006). Synthesis and characterization of phosphorylcholine-substituted chitosans soluble in physiological pH conditions. *Biomacromolecules, 7*, 3151–3156.
Tiera, V. A. O., Tiera, M. J., & Winnik, F. M. (2010). Interaction of amphiphilic derivatives of chitosan with DPPC (1,2-dipalmitoyl-sn-glycero-3-phosphocholine). *Journal of Thermal Analysis and Calorimetry, 100*(1), 309–313.
Yeaman, M. R., & Yount, N. Y. (2003). Mechanisms of antimicrobial peptide action and resistance. *Pharmacological Reviews, 55*, 27–55.